ISBN: 978-3-95450-208-0 doi:10.18429/JACoW-IPAC2019-MOPGW110

STUDY OF THE BEAM CURRENT EFFECTS ON THE NSLS-II STORAGE RING OPTICS USING TURN-BY-TURN DATA*

J. Choi†, Y. Hidaka, Brookhaven National Lab., Upton, New York

Abstract

These days, the techniques using the turn-by-turn data are well developed in analyzing the accelerator optics. We compared the data for the low and high beam currents and studied the beam current effects on the storage ring lattice optics. Also, by comparing the local transfer matrices, we analyzed the amounts of the impacts on the linear optics around the ring.

INTRODUCTION

The National Synchrotron Light Source II (NSLS-II) is a state of the art 3 GeV third generation light source at Brookhaven National Laboratory [1]. NSLS-II storage ring consists of 30 cells and 2 cells are making one supercell. At one end of the supercell there is a long straight section with high β_x and at the other end there is a short straight section with low β_x. Among the long straight sections, 3 places are occupied by damping wigglers (DWs) to reduce the beam emittance.

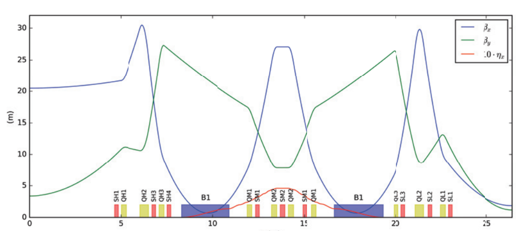

Figure 1: One supercell (2 cell) of NSLS-II storage ring lattice.

As can be seen in Fig. 1, there are three quadrupole families, QH, QL, and QM. Three QHs and three QLs are surrounding high-β_x and low-β_x straight sections, respectively, to match optics. And two QM families are placed in the dispersive region and adjust the optics in the region.

As the measure of machine performance, the Twiss parameters [2] are used and continuous efforts are invested to make the measured values to be closed to the design ones. Various methods are developed in measuring the Twiss parameters [3–6] and the results are considered quite reliable.

Among Twiss parameters, the phase advances using the turn-by-turn data are believed to be hardly affected by the BPM reading errors and, because of their locality, they are used to identify the error sources with the deviations from the design values [7, 8]. We also tried to find the error sources from the differences in phase advances using the design and active models, where the active model is constructed from the conversion table of magnet strengths [9].

However, because the phase advances are not only affected by the local variations at the region but also affected by global variations, the real deviations are embedded in the global fluctuation and it it is not easy to identify them unless the error is very conspicuous.

In this paper, in addition to the phase advances, we also use the response matrix deviations, which depend only on the local parameters, to identify the locations of the error sources. As the measure of matrix differences, the eigen values are used (spectral norm) and, because the lattice is well decoupled, the coupling is not considered. By measuring parameters with different beam currents, about 10 mA and 100 mA, we identified the locations where the optics are heavily affected by the beam current.

MODELS

As usual, the NSLS-II ring has the desired Twiss parameters which are consistent with them of the design model and the machine is continually optimized to have the design parameters.

However, that does not mean all the magnet power supplies are set according to the design lattice file and there can be another model, called as active model in this paper, from the magnet power supply set-point values. Having a reliable active model consistent with the real machine would be very convenient in the operation of the light source because we can calculate the desired lattices and apply them to the machine.

Figure 2 and 3 are showing the differences between the two models. As you can see, even between the analytic models, the difference distributions in phase advance and response matrices have very different characteristics. The injection point is BPM 1 and the The three DWs are located at the positions around BPM 48, 108 and 168. In addition, the large gap dipole magnets are located at three positions, BPM 20-23, BPM 80-83, and BPM 140-143 regions. To be more realistic, we used the design field map for the dipole fringe fields in both models [10].

In phase advances, especially in the vertical plane, broad periodicity of three can be seen and it is not clear how they are generated. It appears that the differences are big at the DW locations. However, from the response matrix differences, we can see the periodicity is coming from the differences except the DWs because the same kick-map file is used for both models. The response matrix differences also vanish at the dipole magnet locations because the active model includes the dipoles with the exactly same methods as the design model.

* Work supported by DOE contract No: DE-SC0012704
† jchoi@bonl.gov

ISBN: 978-3-95450-208-0 doi:10.18429/JACoW-IPAC2019-MOPGW110

MEASUREMENTS

We measure the Twiss parameters for the beam currents of 10 mA and 100 mA and the measured and model tune values are shown in Table 1.

Table 1: Measured and Model Tunes

	Horizontal Tune	Vertical Tune
Measurement (10 mA)	33.180	16.287
Measurement (100 mA)	33.186	16.280
Design Model	33.218	16.239
Active Model	33.178	16.419

Using the measured parameters for 10 mA, we compared the phase advances and response matrices with the design and active model values as shown in (Fig. 4-7). And the differences between 10 mA and 100 mA are shown in Fig. 8 and 9.

Figure 4 and 5 show the differences between design model and the 10 mA measurement. In vertical response matrices, we can see the big differences in the every short straight sections because the design model does not have any consideration about the IDs except the DWs.

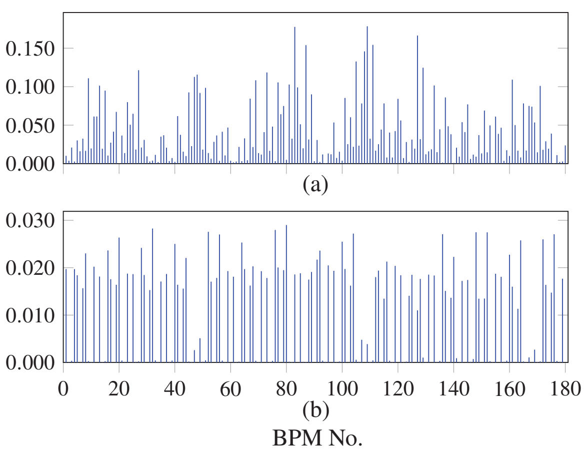

Figure 2: The relative differences in horizontal (a) phase advance and (b) response matrix between the design and the active models.

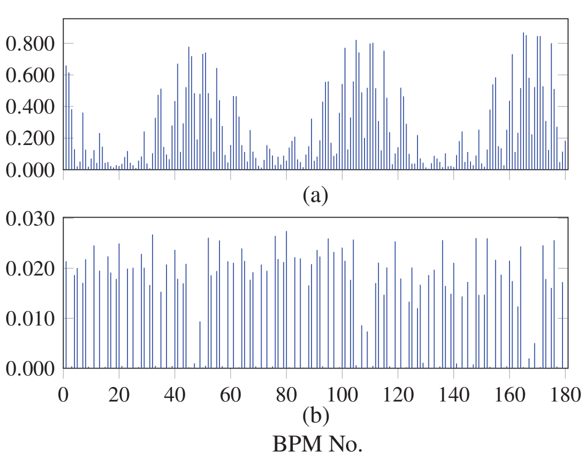

Figure 3: The relative differences in vertical (a) phase advance and (b) response matrix between the design and the active models.

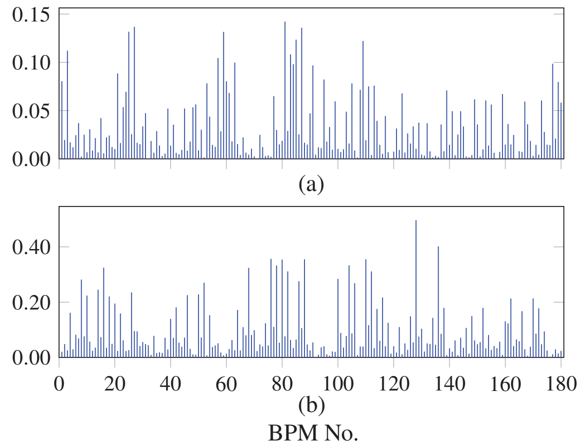

Figure 4: The relative deviations of measured horizontal (a) phase advance and (b) response matrix from the design model for the beam current of 10 mA.

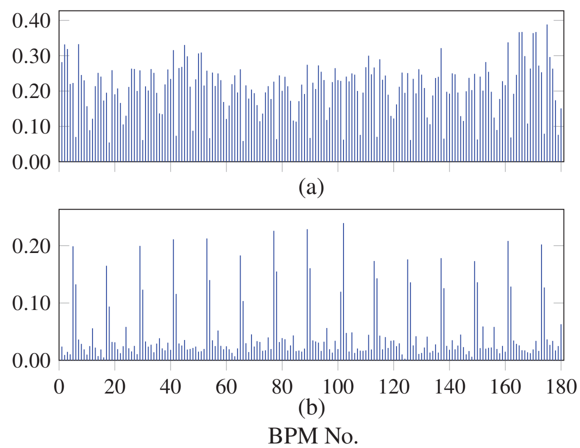

Figure 5: The deviations of measured vertical (a) phase advance and (b) response matrix from the design model for the beam current of 10 mA.

Similarly, the vertical response matrices show differences in short straight sections between the active model and the measurement, but they are lower than the design model case because, even though the ID themselves are not included, the active model lattice is adjusted to compensate the effects from the IDs.

From Fig. 8 and 9, we can see the beam-current effect in the horizontal plane is generally bigger than in the vertical plane and global. But, in the vertical plane, we can identify the cell 17 region is strongly impacted by the beam-current increase compared to other regions.

DISCUSSION

As mentioned, even though the lattice phases can be measure accurately without any model, in measuring other Twiss parameters as well as the response matrices, a model should be involved in some way. Therefore, starting with a good model will be helpful in obtaining reliable measurement data. Because of the limited available turn-by-turn data, the design model tunes have differences from the measured tunes

ISBN: 978-3-95450-208-0 doi:10.18429/JACoW-IPAC2019-MOPGW110

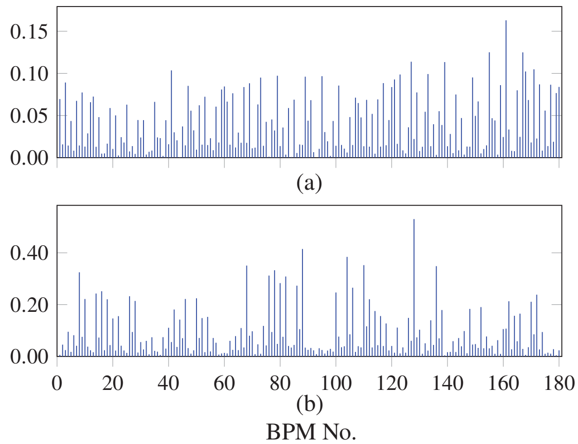

Figure 6: The relative deviations of measured horizontal (a) phase advance and (b) response matrix from the active model for the beam current of 10 mA.

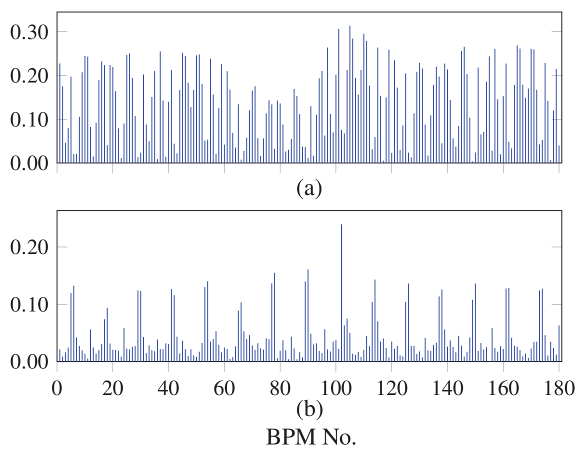

Figure 7: The relative deviations of measured vertical (a) phase advance and (b) response matrix from the active model for the beam current of 10 mA.

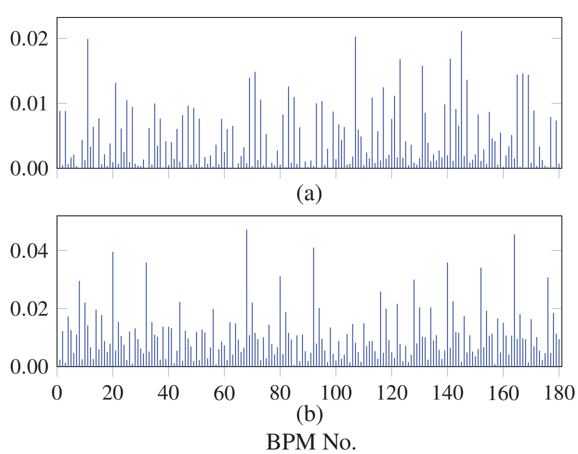

Figure 8: The relative differences in horizontal (a) phase advance and (b) response matrix between 10 mA and 100 mA stored ring.

with 10 mA beam-current and they are closer to 100 mA measurements. Still, we applied the design model to 10 mA measurement first because the usual optimization processes are performed with the low beam currents. However, the

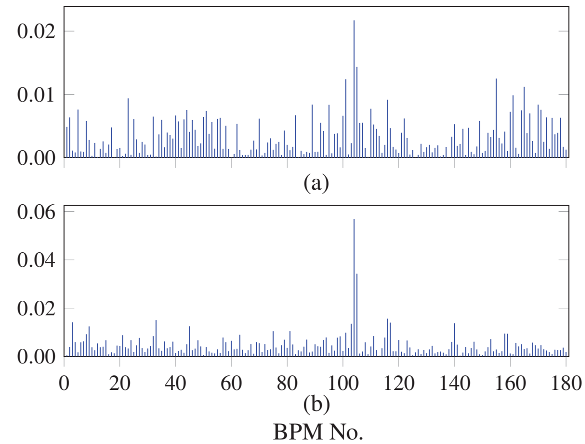

Figure 9: The relative differences in vertical (a) phase advance and (b) response matrix between 10 mA and 100 mA stored ring.

model is not considered to affect the results of the differences between the 10 mA and 100 mA lattices.

Because of the lack of enough consistency between the design model and the measurements, the study is focussed on identifying the effects from the beam current. If we have well-tuned lattice to the design model, the measured response matrices can be used to correct the active model and the directly applicable active model could be available.

REFERENCES

[1] G. M. Wang and Y. Hidaka, "Experience From First Four Years of NSLS-II Operations", presented at the 10th Int. Particle Accelerator Conf. (IPAC'19), Melbourne, Australia, May 2019, paper TUPGW104, this conference.

[2] E. D. Courant, H. S. Snyder, "Theory of the Alternating-Gradient Synchrotron," *Annals of Physics*, Vol. 3 (1958) p.1.

[3] J. Safranek, "Experimental Determination of Storage Ring Optics using Orbit Response Measurements," *Nucl. Instr. and Methods*, A 388 (1997) p.27.

[4] P. Castro *et al.*, "Betatron Function Measurement at LEP Using the BOM 1000 Turns Facility", in *Proc. 15th Particle Accelerator Conf. (PAC'93)*, Washington D.C., USA, Mar. 1993, pp. 2103–2106.

[5] C. Wang, V. Sajaev, C. Yao, "Phase Advance and β Function Measurements using Model-Independent Analysis," *Phys. Rev. ST* Vol.6, 104001, (2003)

[6] A. V. Petrenko, V. A. Lebedev, and A. Valishev, "Independent Component Analysis of Tevatron Turn-by-turn BPM Measurements", in *Proc. 11th European Particle Accelerator Conf. (EPAC'08)*, Genoa, Italy, Jun. 2008, paper WEPP037, pp. 2602–2604.

[7] D. Brandt *et al.*, "Measurements of Impedance Distributions and Instability Thresholds in LEP", in *Proc. 16th Particle Accelerator Conf. (PAC'95)*, Dallas, TX, USA, May 1995, paper RAA20, p.570.

[8] V. Sajaev, "Transverse Impedance Distribution Measurements Using Response Matrix Fit Method at APS", in *Proc. 20th Particle Accelerator Conf. (PAC'03)*, Portland, OR, USA, May 2003, paper WOAB011, p.417.

ISBN: 978-3-95450-208-0 doi:10.18429/JACoW-IPAC2019-MOPGW110

[9] J. Choi, W. Guo, T. V. Shaftan, and X. Yang, "Reproducibility Issues of NSLS-II Storage Ring and Modeling of the Lattice", in *Proc. IPAC'17*, Copenhagen, Denmark, May 2017, pp. 2851–2853. doi:10.18429/JACoW-IPAC2017-WEPAB120

[10] J. Choi, Y. Hidaka, T. V. Shaftan, C. J. Spataro, and G. M. Wang, "Dipole Fringe Field Analysis of the NSLS-II Storage Ring", in *Proc. IPAC'18*, Vancouver, Canada, Apr.-May 2018, pp. 1519–1521. doi:10.18429/JACoW-IPAC2018-TUPMK014